

## Article

# Acquisition Conditions for Lu-177 DOTATATE Imaging

Yuri Sagisaka <sup>1,\*</sup>, Yasuyuki Takahashi <sup>1,\*</sup>, Shota Hosokawa <sup>1</sup>, Niina Kanazawa <sup>2</sup>, Hiroki Yamamoto <sup>3</sup>, Go Takai <sup>4</sup> and Keiji Nagano <sup>5</sup>

<sup>1</sup> Department of Radiation Science, Graduate School of Health Sciences, Hirosaki University, 66-1 Hon-cho, Hirosaki 036-8564, Japan; shosokawa@hirosaki-u.ac.jp

<sup>2</sup> Department of Radiological Technology, Nihon University Itabashi Hospital, 30-1 Oyaguchi kami-cho Itabashi-ku, Tokyo 173-8610, Japan

<sup>3</sup> Department of Radiology, Division of Medical Technology, Hirosaki University Hospital, 53 Hon-cho, Hirosaki 036-8563, Japan; hyamamoto@hirosaki-u.ac.jp

<sup>4</sup> Department of Radiological Technology, Division of Radiology, Kansai Electric Power Hospital, 2-1-7 Fukushima Fukushima-ku, Osaka 553-0003, Japan; takai.go@b4.kepco.co.jp

<sup>5</sup> Division of Radiation Management Center, Dokkyo Medical University Hospital, 880 Kitakobayashi, Mibumachi, Shimotsuga-gun, Tochigi 321-0293, Japan; k-nagano462@dokkyomed.ac.jp

\* Correspondence: yuri.s806@gmail.com (Y.S.); ytaka3@hirosaki-u.ac.jp (Y.T.); Tel.: +81-172-33-5111 (Y.T.)

**Simple Summary:** We aimed to image the distribution of lutetium oxodotreotide in the body, which is used in peptide receptor radionuclide therapy. We investigated imaging conditions using gamma rays emitted from the radionuclide. The energy peaks of the gamma rays were 56, 113, and 208 keV. We compared image quality by combining imaging from low–medium-energy general-purpose (LMEGP) and medium-energy general-purpose collimators (MEGP). In phantom studies, static and SPECT images showed that the combination of 56, 113, and 208 keV (three peaks) and LMEGP yielded the best count ratio and image quality results based on visual evaluation, count ratios, and recovery coefficient (RC) curves.

**Abstract:** We investigated imaging conditions for the distribution of lutetium oxodotreotide (Lu-177 DOTATATE) in the body during peptide receptor radionuclide therapy for neuroendocrine tumor (NET). We investigated imaging conditions using gamma rays emitted from the radionuclide. The gamma rays had energy peaks at 113 and 208 keV and characteristic X-rays at 56 keV. Image quality was compared by utilizing a combination of low–medium-energy general-purpose (LMEGP) and medium-energy general-purpose (MEGP) collimators. This study included the measurement of total spatial resolution (Full Width at Half Maximum) using a line source phantom. We compared the image quality of static images using a plane phantom and SPECT images using a cylindrical phantom. This comparison involved assessing recovery coefficient curves, count ratio, and %CV. Imaging evaluation was also performed on one NET patient. In phantom studies and the clinical study, comparing the combination of the three energy peaks (56 + 113 + 208 keV) using the LMEGP collimator and the conventional combination (113 + 208 keV) using the MEGP collimator revealed a count ratio of 1.9 times the maximum, stable %CV, and the best image quality.

**Keywords:** LMEGP collimator; three peaks; MEGP collimator; two peaks; Lu-177



**Citation:** Sagisaka, Y.; Takahashi, Y.; Hosokawa, S.; Kanazawa, N.; Yamamoto, H.; Takai, G.; Nagano, K. Acquisition Conditions for Lu-177 DOTATATE Imaging. *Radiation* **2024**, *4*, 17–25. <https://doi.org/10.3390/radiation4010002>

Academic Editor: Ehsan Nazemi

Received: 6 December 2023

Revised: 13 January 2024

Accepted: 16 January 2024

Published: 19 January 2024



**Copyright:** © 2024 by the authors. Licensee MDPI, Basel, Switzerland. This article is an open access article distributed under the terms and conditions of the Creative Commons Attribution (CC BY) license (<https://creativecommons.org/licenses/by/4.0/>).

## 1. Introduction

Peptide receptor radionuclide therapy using lutetium oxodotreotide (Lu-177 DOTATATE) for neuroendocrine tumor (NET) treatment was approved in Japan in June 2021 [1,2]. Somatostatin receptor (SSTR) is expressed in NETs in more than 80% of cases. Lu-177 DOTATATE is a radionuclide that specifically binds to SSTR and can selectively treat tumor cells [3]. Lu-177 uses emitted beta rays to treat tumor cells but also emits gamma rays, making it possible to obtain scintigram images with a gamma camera. Most imaging studies reported a combination of a medium-energy general-purpose (MEGP) collimator and two energy

peaks at 113 + 208 keV [4,5]. We noted that the Tl-201 Cl image uses a characteristic X-ray of 71 keV [6]. Lu-177 also has an energy peak of characteristic X-rays; however, it was not utilized. In the Table of Radioactive Isotopes [7], the main photon energies and emission rates from Lu-177 are 11.0% at 208 keV, 6.4% at 113 keV, 4.5% at 55.5 keV (Hf-K $\alpha$ ), and 1.2% at 63.7 keV (Hf-K $\beta$ ). Its energy spectrum using a low–medium-energy collimator is shown in Figure 1. Due to the low energy resolution of the gamma camera, the characteristic X-ray energy peaks of 55.5 keV and 63.7 keV overlap and appear as a single peak at 56.0 keV. However, the detection efficiency of the NaI (Tl) scintillator is large (56.0 keV), and the energy spectrum is different in the performance of the collimators (Figure 1). A low–medium-energy general-purpose (LMEGP)-type [8,9] collimator is used for In-111 pentetate in somatostatin receptor scintigraphy (SRS) imaging. The acquisition condition for Lu-177 imaging consists of a combination of a MEGP collimator and one peak (208 keV) or two peaks (113 keV and 208 keV). To the best of our knowledge, no previous study has reported an LMEGP collimator with a wide energy range and three peaks (56, 113, and 208 keV), including the characteristic X-ray of 56 keV.

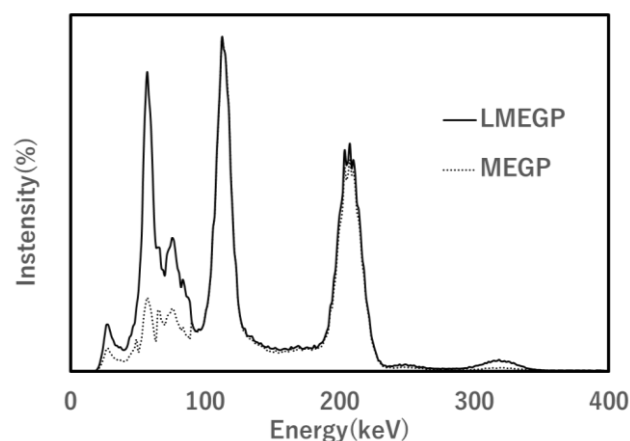


**Figure 1.** Energy spectrum for Lutetium-177 of each collimator. Solid line is low–medium-energy general-purpose (LMEGP) collimator, and dotted line is medium-energy general-purpose (MEGP) collimator.

In this study, we reviewed the appropriate acquisition conditions for Lu-177 images.

## 2. Materials and Methods

### 2.1. System Condition

The SPECT system used was a Symbia T-6 (SIEMENS Healthcare, Bayerm, Germany) with CT device. We used e.soft data processors. The energy window was 56, 113, and 208 keV with a window width of 20%. The energy peaks were acquired separately and compared in combination with image processing. The combined energy peaks are 113 + 208 keV and 56 + 113 + 208 keV. Two different collimator combinations, LMEGP and MEGP, were also compared.

### 2.2. Total Spatial Resolution

The total spatial resolution (Full Width at Half Maximum (FWHM)) with the Lu-177 source phantom (diameter: 1 mm) was measured according to the NEMA standard [10]. However, the radioactivity concentration of the line source is weak, and the acquisition time is very long; thus, only static images without scatterers (water) were measured for FWHM.

### 2.3. Phantom Study

Two types of liver phantoms were created—one was an original plane phantom for static images, and the other was a cylindrical phantom for SPECT images.

### 2.3.1. Static Images

Static images were used instead of whole-body images. The size of the original plane phantom was 10 cm × 30 cm. Imitation tumors (signals) with diameters of 7, 10, 15, 20, and 30 mm were placed 5 cm equidistant (Figure 2a). BG (liver) was set to 200 kBq/mL with reference to the accumulation ratio of In-111 pentetreotide [9,10], and the imitated tumor was set to five times for the plane phantom. The imaging conditions were a matrix size of 256 × 256 and acquisition time of 5 min.

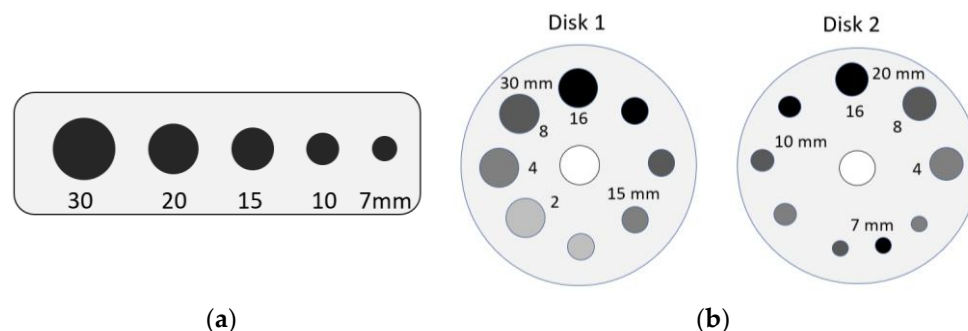


**Figure 2.** Signal position inside the phantom. (a) Static phantom, (b) SPECT phantom. (b) Simulated tumors were set at 2-, 4-, 8-, and 16-fold concentrations and are shown in light gray.

### 2.3.2. SPECT Images

In SPECT, the cylindrical phantom (JS-10, Kyoto-Kagaku, Japan) was 250 mm in diameter and 300 mm in length. Imitation tumors (signals) were placed concentrically from the center (Figure 2b). The radioactivity concentration ratio of the signal (2, 4, 8, and 16 times the BG (liver)) was set to 200 kBq/mL with reference to the accumulation ratio of In-111 pentetreotide [11,12].

SPECT data were acquired in a matrix size of 128 × 128 in continuous mode (5 min/rotation) with three repeated rotations at 6° intervals (60 directions, 360° acquisition/detector). The projection data were added for each rotation to configure 5, 10, and 15 min data. The ordered subset-expectation maximization (OS-EM) method was used for SPECT image reconstruction (iteration times 10, 5 subsets). The image-correction methods used were the dual energy window subtraction scatter correction method for scatter correction and CT-based attenuation correction method.

### 2.4. Human Study

As a human study, a 35-year-old male patient with NET diagnosed on the basis of clinical and CT findings was evaluated. Twenty-four hours after the intravenous injection of 7.4 GBq of Lu-177 DOTATATE, whole-body images and SPECT images were acquired. Whole-body images were acquired with a matrix size of 256 × 1024 at scan speed of 20 cm/min. SPECT-acquisition conditions were the same as for the phantoms. We used the LMEGP collimator according to the code of ethics. We obtained energy peaks separately for 56, 113, and 208 keV and compared them in combination. This study was approved by the Ethics Committee of Kansai Electric Power Hospital (21-101). Two energy peaks and three energy peaks images are possible with image processing after one imaging. Comparison of two or three energy peaks on the MEGP collimator is necessary; however, the Ethics Committee did not approve twice imaging as it would increase the physical and mental stress on the patient.

### 2.5. Statistics

Static images were evaluated using count ratio (maximum counts) and recovery coefficient (RC) curve.

SPECT images were evaluated by visual evaluation including differences in acquisition time, count ratio (maximum counts and average counts), RC curve, and %CV. Signals of

SPECT images were compared at maximum counts. Each image was standardized to a maximum count of 100%, and the relationship with the signal size was calculated as RC (Formula (1)):

$$RC_j = \frac{C_j}{C_{30\text{mm}}} \times 100 (\%) \quad (1)$$

where  $C_j$  represents the maximum number of counts in each sphere, and  $C_{30\text{mm}}$  is the maximum number of counts within ROI of 30 mm sphere. In addition, the %CV of image quality was calculated (Formula (2)):

$$\%CV = \frac{SD_{BG}}{C_{BG}} \times 100 (\%) \quad (2)$$

where  $C_{BG}$  represents the average count within ROI in BG, and  $SD_{BG}$  is the standard deviation within ROI in BG.

The energy peak of 113 + 208 keV is indicated as two peaks, and the energy peak of 56 + 113 + 208 keV is indicated as three peaks. When in combination with each collimator, it is indicated as two peaks + LMEGP, two peaks + MEGP, three peaks + LMEGP, and three peaks + MEGP.

### 3. Results

#### 3.1. Total Spatial Resolution

The FWHM were 11.82 mm for two peaks + LMEGP, 9.05 mm for three peaks + LMEGP, 9.69 mm for two peaks + MEGP, and 8.62 mm for three peaks + MEGP.

#### 3.2. Phantom Study

##### 3.2.1. Static Image

Static images with different combinations of energy peaks and collimators are shown in Figure 3. The count ratio (maximum value) and RC curve are shown in Figures 4a and 4b, respectively.

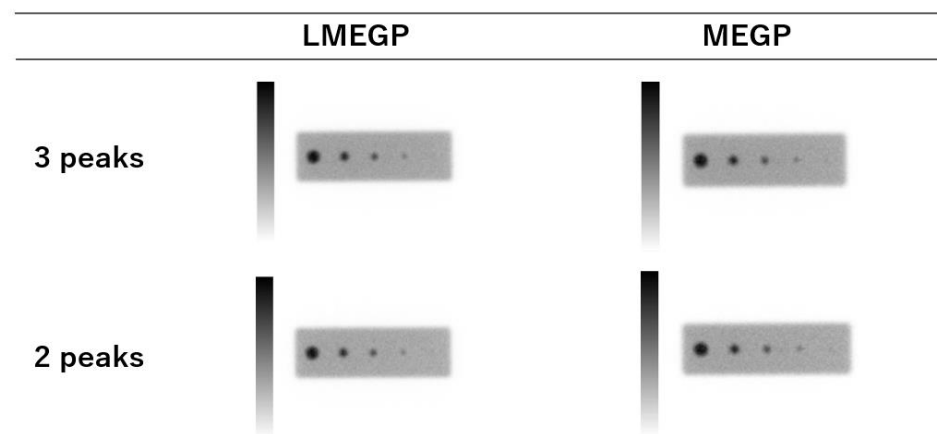


**Figure 3.** Static image for each imaging condition. Upper row is three peaks (56 + 113 + 208 keV) imaging, and lower row is two peaks (113 + 208 keV) imaging. LMEGP collimator is on the left, and MEGP collimator is on the right.

The visual evaluation showed similar signal detectability with a size of 15 mm, taking into account the resolution of the gamma camera. Three peaks + LMEGP was 1.8 times more counts than the conventional imaging method (two peaks + MEGP). In the RC curve, three peaks + LMEGP was best, with a maximum 1.1 times difference compared to the conventional imaging method. The %CV was 6.1% for three peaks + LMEGP, 5.9% for three peaks + MEGP, 6.6% for two peaks + LMEGP, and 6.8% for two peaks + MEGP. Thus, three peaks + MEGP was slightly stable.

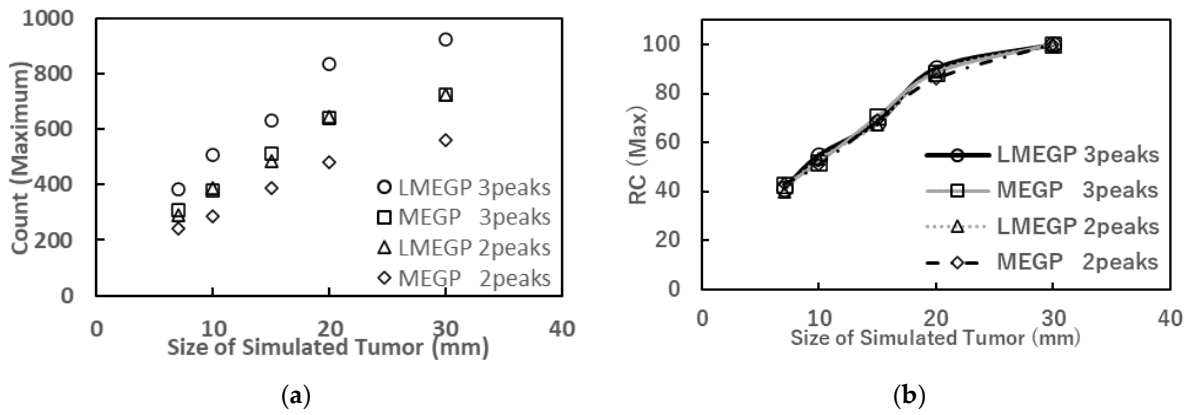


**Figure 4.** Image analysis of static images. (a) Maximum count ratio: X-axis is the signal size, and Y-axis is the maximum count for each imaging condition. (b) RC curve: X-axis is the signal size, and Y-axis is the normalizing count for each imaging condition.

3.2.2. SPECT Image

SPECT images with different combinations of energy peaks and collimators are shown in Figure 5. The count ratio (maximum value) and RC curve are shown in Figures 6a and 6b, respectively.

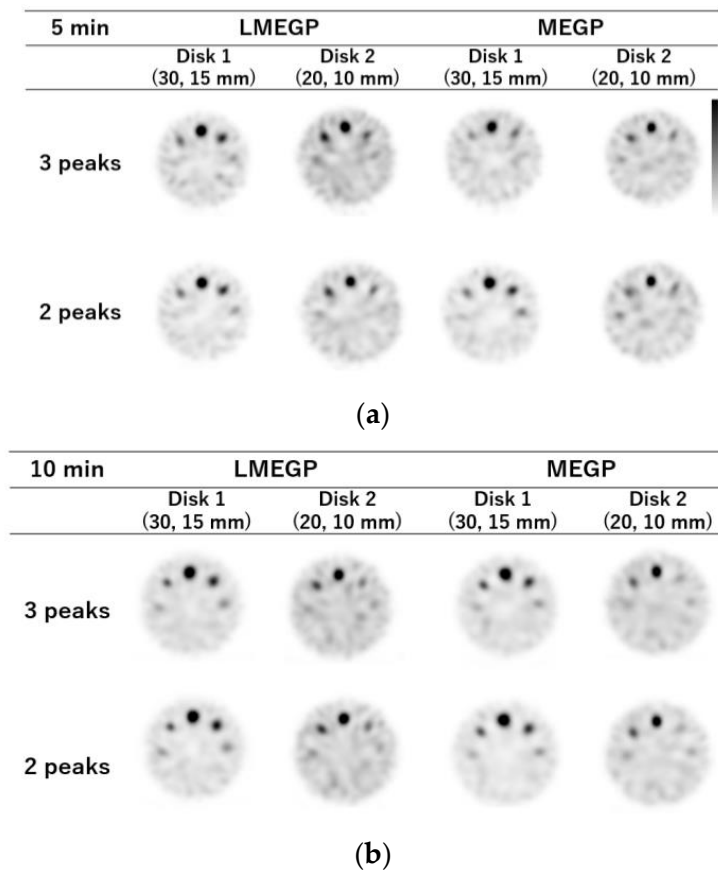


**Figure 5.** Cont.

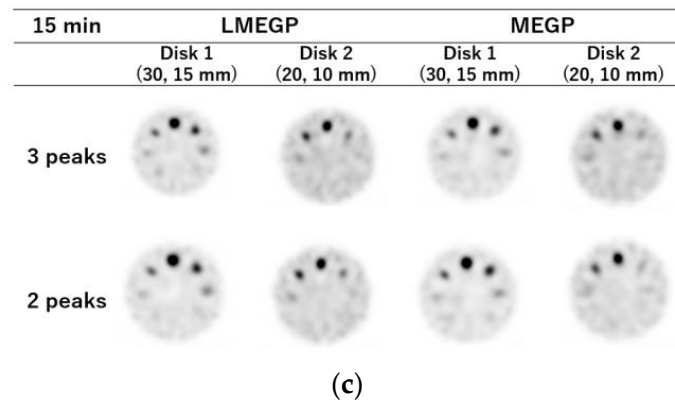


**Figure 5.** Static image for each imaging condition; (a) 5 min images; (b) 10 min images; (c) 15 min images. The radioactivity concentration ratio, size, and position of the signals are shown in Figure 2b.

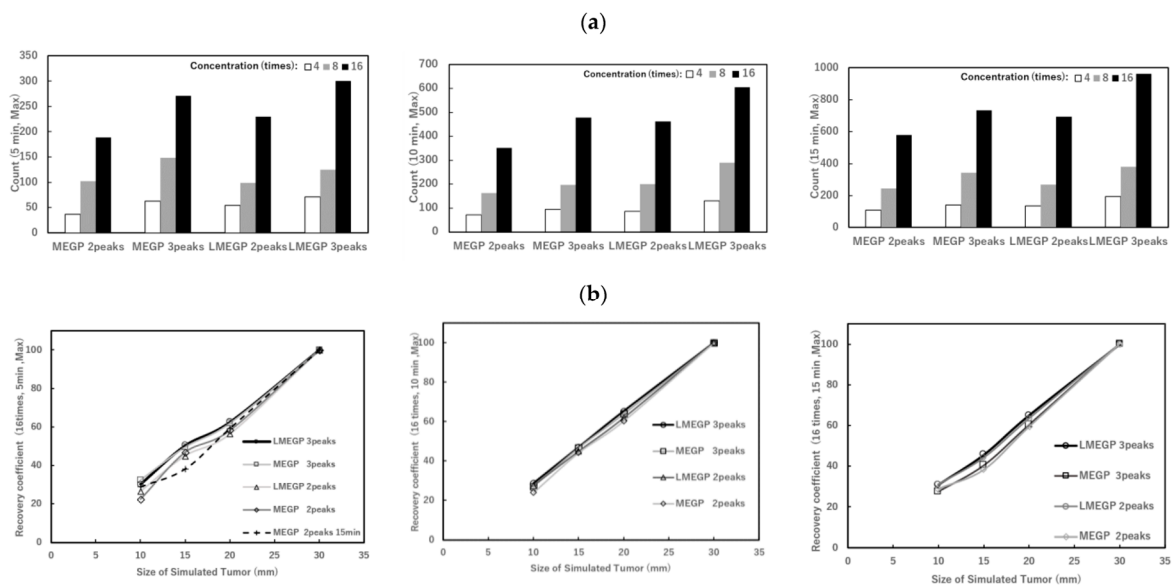


**Figure 6.** Maximum count for each imaging condition at each radioactivity concentration. (a) and (b) both show results for 5, 10, and 15 min imaging from top to bottom. (a) Maximum count ratio: X-axis is the signal size, and Y-axis is the maximum count for each imaging condition. (b) RC curve: X-axis is the signal size, and Y-axis is the normalizing count for each imaging condition.

The visual evaluation revealed that the 10 min imaging of three peaks + LMEGP had a radioactivity concentration four times that of 30 mm, eight times that of 20 mm, and a circular shape. Greater distortion was observed in Disk 2 at 5 min imaging than the conventional imaging method (Figure 5).

The count ratios of three peaks + LMEGP were higher than those of the conventional two peaks + MEGP; in particular, regarding the 15 mm signal at the four times concentration (Figure 6a), the radioactivity concentration was 1.9 times at 5 min, 1.8 times at 10 min, and 1.8 times at 15 min, showing an increase. In the RC curve, the curve of three peaks + LMEGP was large (Figure 6b). In Figure 6b, for 5 min imaging, two peaks + MEGP for the 15 min imaging is shown as a dotted line to compare with the conventional condition. This result indicates that the RC curve of three peaks + LMEGP for 5 min imaging is better than that of two peaks + MEGP for 15 min imaging.

### 3.2.3. Human Study

Due to ethical regulations, the collimator was used only for LMEGP to reduce the effect on the mental health of the patient. Visual evaluations based on differences in the number of energy peaks were almost the same (Figure 7).

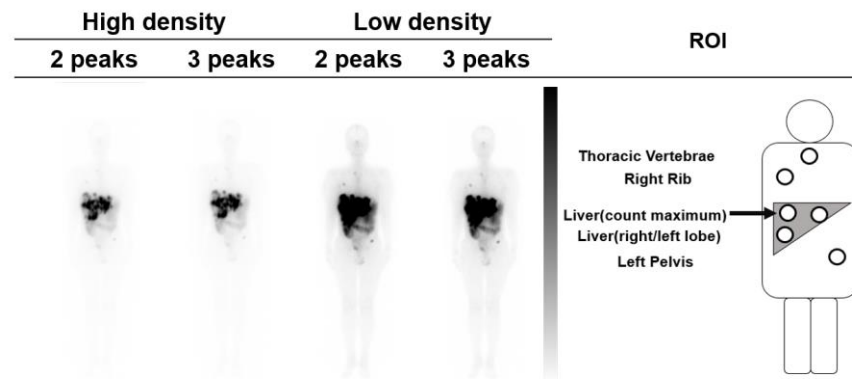


**Figure 7.** A case of NET. The left is high density, the center is low density, and the right is the ROI position.

The accumulation counts of Lu-177 DOTATATE were compared using the following ROIs (Figure 7, right): multiple liver metastases (a), right anterior superior area: S8 (b), left lateral superior area: S2 (c), thoracic (d), right rib (e), and left pelvis (f). The accumulation count of three peaks + LMEGP increased in all areas from low to high accumulation (Figure 8), with a maximum 1.5-times increase in counts at the left pelvis.

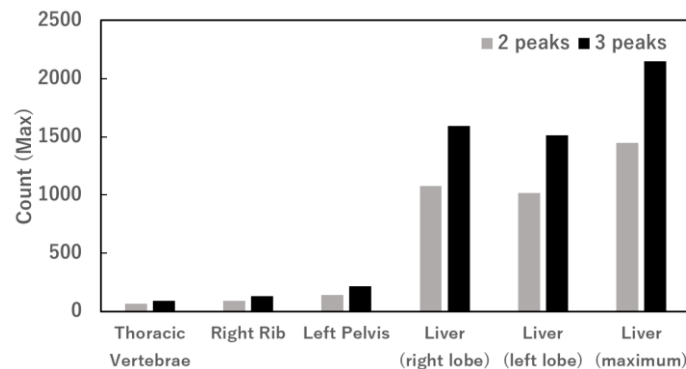


**Figure 8.** Maximum count within ROI of a clinical case. X-axis is the ROI position, and Y-axis is the maximum count within the ROI.

#### 4. Discussion

NET is a general term for tumors arising from neuroendocrine cells. NET can occur in all organs of the body, but the pancreas, gastrointestinal tract, and lungs account for 80% of cases [13]. It is classified into three types: highly differentiated (NET); poorly differentiated (NEC); and MiNEN, which is a mixture of NET or NEC and cancer cells. In Europe and the U.S., midgut NET is more common, but in Japan, NET of the colon and rectum is more common. NET therapy options include surgery, pharmacotherapy, and internal RI therapy. As SSTRs are expressed on NETs in more than 80% of cases [2,14], peptide receptor radionuclide therapy is used for treatment. Lu-177 uses emitted beta rays to treat tumor cells. The maximum dose is 7.4 GBq per infusion administered intravenously up to four times at 8-week intervals [2,15]. The maximum energy of  $\beta$ -rays is 498 keV, and the maximum range is 2.2 mm, which irradiates the tumor while minimizing damage to surrounding tissues. Moreover, Lu-177 emits gamma rays, making it possible to obtain scintigram images with a gamma camera.

Lu-177 DOTATATE scintigraphy focuses on energy peaks and collimators. The characteristic X-ray used for Lu-177 is 56 keV [7]. Huizing et al. reported a combination of 113 + 208 keV [5]. Furthermore, Roth et al. investigated the usefulness of 56, 113, and 208 keV peaks for semiconductor gamma cameras [16]; however, they have not been applied clinically.

In the present study, we used an LMEGP-type collimator with a target energy of 190 keV or less and an MEGP-type collimator with a target energy in the range of 160 to 300 keV. Although

the energy peak of 56 keV has a lower passage rate in MEGP (Figure 1), it is clearly detected in LMEGP. However, the energy range varies slightly depending on the manufacturer. The analysis method was based on the maximum value and took variation in counts into account.

Therapy of NET patients with Lu-177 DOTATATE is accompanied by mental and physical considerations. In addition, confirmation of therapeutic efficacy by Lu-177 DOTATATE scintigraphy is often difficult. Increasing the acquisition counts can shorten acquisition time and affect the mental health of patients. For these reasons, we reviewed the combination of energy peaks, considering LMEGP collimators, to increase the number of acquired counts.

In the phantom studies, the image quality was the same, and the count increased in the LMEGP and three-peak combination condition compared to the conventional MELP and two-peak combination condition. The RC curve and %CV were the best when we investigated the combined conditions of LMEGP and three peaks. These results suggest that this imaging condition increases the count and improves SN, thereby improving the recognition of small tumors. Furthermore, conventional scintigraphy uses static or whole-body imaging, but SPECT may also be added.

The therapeutic effect of Lu-177 DOTATATE has been measured by morphological imaging criteria or functional imaging using Gallium-DOTA peptide studies (Ga-68 DOTATATE) or somatostatin analogue scintigraphy (In-111 pentetreotide) [17]. Ga-68 DOTATATE PET/CT is superior to In-111 pentetreotide in image quality and quantitation [18]. However, Ga-68 DOTATATE PET/CT is only available in a limited number of hospitals in Japan. Lu-177 DOTATATE imaging reflects the distribution of the metabolic therapy received; in addition, it is performed in multiple doses at fixed intervals, enabling the evaluation of risk organs by imaging at each time. Therefore, this imaging could be used for theranostics [19].

## 5. Conclusions

The LMEGP collimator showed a wider energy range and increased counts when used in combination with the LMEGP 3 peak. It is thought that the increase in counts with 3 peaks results in better SN and allows for better visibility of small tumors.

The results of this experiment showed that MEGP + 2 peaks with 15 min imaging was equivalent in image quality to LMEGP + 3 peaks with 5 min imaging, suggesting that the examination time can be shortened and the examination burden on the patient can be reduced. Further study of imaging time is required to expand the possibilities of imaging conditions for LMEGP + 3 peaks.

**Author Contributions:** Conceptualization, Y.S. and Y.T.; methodology, Y.T.; investigation, Y.S. and Y.T.; writing—original draft preparation, Y.S.; writing—review and editing, S.H., N.K., H.Y., G.T. and K.N.; supervision, Y.S. and Y.T.; project administration, Y.S. and Y.T. All authors have read and agreed to the published version of the manuscript.

**Funding:** This research received no external funding.

**Institutional Review Board Statement:** The study was conducted in accordance with the Declaration of Helsinki, and approved by the Institutional Review Board (or Ethics Committee) of Kansai Electric Power Hospital (no. 21-101, approved on 28 January 2022).

**Informed Consent Statement:** This study used anonymized data. The explanation and consent of the study were posted on the information board.

**Data Availability Statement:** The data presented in this study are available in this article.

**Conflicts of Interest:** The authors declare no conflicts of interest.

## References

1. Hosono, M.; Ikebuchi, H.; Nakamura, Y.; Nakamura, N.; Yamada, T.; Yanagida, S.; Kitaoka, A.; Kojima, K.; Sugano, H.; Kinuya, S.; et al. Manual on the proper use of lutetium-177-labeled somatostatin analogue (Lu-177-DOTA-TATE) injectable in radionuclide therapy (2nd ed.). *Ann. Nucl. Med.* **2018**, *32*, 217–235. [[CrossRef](#)] [[PubMed](#)]
2. Kawata, T. Radiopharmaceuticals/Peptide Receptor Radionuclide Therapeutics, LUTATHERA<sup>®</sup> Injection, Lutetium (<sup>177</sup>Lu) oxodotreotide. *Drug Deliv. Syst.* **2023**, *38*, 165–170. [[CrossRef](#)]
3. Oberg, K.; Kvols, L.; Caplin, M.; Delle Fave, G.; de Herder, W.; Rindi, G.; Ruzsniowski, P.; Woltering, E.A.; Wiedenmann, B. Consensus report on the use of somatostatin analogs for the management of neuroendocrine tumors of the gastroenteropancreatic system. *Ann. Oncol.* **2004**, *15*, 966–973. [[CrossRef](#)] [[PubMed](#)]
4. Asmi, H.; Bentayeb, F.; Bouzekraoui, Y.; Bonutti, F.; Douama, S. Energy Window and Collimator Optimization in Lutetium-177 Single-photon Emission Computed Tomography Imaging using Monte Carlo Simulation. *Indian J. Nucl. Med.* **2020**, *35*, 36–39.
5. Huizing, D.M.V.; Sinaasappel, M.; Dekker, M.C.; Stokkel, M.P.M.; de Wit-van der Veen, B.J. <sup>177</sup>Lu Lutetium SPECT/CT: Evaluation of collimator, photopeak and scatter correction. *J. Appl. Clin. Med. Phys.* **2020**, *21*, 272–277. [[CrossRef](#)]
6. Kojima, A.; Takagi, A.; Noguchi, T.; Matsumoto, M.; Katsuda, N.; Tomiguchi, S.; Yamashita, Y. Optimum energy window setting on Hg-201 x-rays photopeak for effective Tl-201 imaging. *Ann. Nucl. Med.* **2005**, *19*, 541–547. [[CrossRef](#)] [[PubMed](#)]
7. Chu, S.Y.F.; Ekström, L.P.; Firestone, R.B. Table of Isotopes. Database Version 1999-02-28. Available online: <http://nucleardata.nuclear.lu.se/toi/nuclide.asp?iZA=710177> (accessed on 2 October 2023).
8. Kanzaki, T.; Takahashi, Y.; Higuchi, T.; Zhang, X.; Mogi, N.; Suto, T.; Tsushima, Y. Evaluation of a Correction Method for <sup>111</sup>In-Pentetreotide SPECT Imaging of Gastroenteropancreatic Neuroendocrine Tumors. *J. Nucl. Med. Tech.* **2020**, *48*, 326–330. [[CrossRef](#)] [[PubMed](#)]
9. Yamashita, K.; Miyaji, N.; Motegi, K.; Terauchi, T.; Ito, S. Development of a new quantification method using partial volume effect correction for individual energy peaks in <sup>111</sup>In-pentetreotide SPECT/CT. *Asia Ocean. J. Nucl. Med. Biol.* **2022**, *10*, 126–137. [[CrossRef](#)]
10. National Electrical Manufacturers Association. *Performance Measurements of Gamma Cameras NEMA Standards Publication NU 1-2018*; National Electrical Manufacturers Association: Rosslyn, VA, USA, 2019; pp. 42–46.
11. Inoue, T.; Ootake, H.; Hirano, T.; Tomiyoshi, K.; Endo, K.; Tanaka, K.; Shimizu, N.; Saito, T. Pharmacokinetics and dosimetry of the somatostatin analog <sup>111</sup>In-DTPA-D-Phe-Octreotide -Report of the phase 1 study-. *Jpn. J. Nucl. Med. (KAKUIGAKU)* **1995**, *32*, 511–521. (In Japanese)
12. Öhrvall, U.; Westlin, J.E.; Nilsson, S.; Wilander, E.; Juhlin, C.; Rastad, J.; Akerström, G. Human Biodistribution of [<sup>111</sup>In]Diethylenetriamine-pentaacetic Acid-(DTPA)-D-[Phe<sup>1</sup>]-octreotide and peroperative detection of endocrine tumors. *Cancer Res.* **1995**, *55* (Suppl. 23), 5794s–5800s. [[PubMed](#)]
13. Kwekkeboom, D.J.; Teunissen, J.J.; Bakker, W.H.; Kooij, P.P.; de Herder, W.W.; Feelders, R.A.; van Eijck, C.H.; Esser, J.P.; Kam, B.L.; Krenning, E.P. Radiolabeled Somatostatin Analog [<sup>177</sup>Lu-DOTA<sup>0</sup>, Tyr<sup>3</sup>]Octreotate in Patients with Endocrine Gastroenteropancreatic Tumors. *J. Clin. Oncol.* **2005**, *23*, 2754–2762. [[CrossRef](#)] [[PubMed](#)]
14. Tsuta, K.; Wistuba, I.I.; Moran, C.A. Differential expression of somatostatin receptors 1-5 in neuroendocrine carcinoma of the lung. *Rathol. Res. Pract.* **2012**, *208*, 470–474. [[CrossRef](#)] [[PubMed](#)]
15. Ito, T.; Igarashi, H.; Nakamura, K.; Sasano, H.; Okusaka, T.; Takano, K.; Komoto, I.; Tanaka, M.; Imamura, M.; Jensen, R.T.; et al. Epidemiological trends of pancreatic and gastrointestinal neuroendocrine tumors in Japan: A nationwide survey analysis. *J. Gastroenterol.* **2015**, *50*, 58–64. [[CrossRef](#)] [[PubMed](#)]
16. Roth, D.; Larsson, E.; Sundlöf, A.; Sjögreen Gleisner, K. Characterisation of a hand-held CZT-based gamma camera for <sup>177</sup>Lu imaging. *EJNMMI Phys.* **2020**, *7*, 46. [[CrossRef](#)] [[PubMed](#)]
17. Kelkar, S.S.; Reineke, T.M. Theranostics: Combining imaging and therapy. *Bioconjug. Chem.* **2011**, *22*, 1879–1903. [[CrossRef](#)] [[PubMed](#)]
18. Sharma, R.; Wang, W.M.; Yusuf, S.; Evans, J.; Ramaswami, R.; Wernig, F.; Frilling, A.; Mauri, F.; Al-Nahhas, A.; Aboagye, E.O.; et al. Ga-DOTATATE PET/CT parameters predict response to peptide receptor radionuclide therapy in neuroendocrine tumours. *Radiother. Oncol.* **2019**, *141*, 108–115. [[CrossRef](#)] [[PubMed](#)]
19. Duan, H.; Igaru, A.; Aparici, C.M. Radiotheranostics—Precision Medicine in Nuclear Medicine and Molecular Imaging. *Nanotheranostics* **2022**, *6*, 103–117. [[CrossRef](#)] [[PubMed](#)]

**Disclaimer/Publisher's Note:** The statements, opinions and data contained in all publications are solely those of the individual author(s) and contributor(s) and not of MDPI and/or the editor(s). MDPI and/or the editor(s) disclaim responsibility for any injury to people or property resulting from any ideas, methods, instructions or products referred to in the content.